Durham University

Durham Research Online

Deposited in DRO:

22 October 2021

Version of attached file:

Published Version

Peer-review status of attached file:

Peer-reviewed

Citation for published item:

Ngwaka, Ugochukwu and Smallbone, Andrew and Jia, Boru and Lawrence, Christopher and Towell, Ben and Roy, Sumit and KV, Shivaprasad and Roskilly, Anthony Paul (2021) 'Evaluation of performance characteristics of a novel hydrogen-fuelled free-piston engine generator.', International Journal of Hydrogen Energy, 46 (66). pp. 33314-33324.

Further information on publisher's website:

https://doi.org/10.1016/j.ijhydene.2020.02.072

Publisher's copyright statement:

This is an open access article distributed under the terms of the Creative Commons CC-BY license, which permits unrestricted use, distribution, and reproduction in any medium, provided the original work is properly cited.

Additional information:

Use policy

The full-text may be used and/or reproduced, and given to third parties in any format or medium, without prior permission or charge, for personal research or study, educational, or not-for-profit purposes provided that:

- a full bibliographic reference is made to the original source
- a link is made to the metadata record in DRO
- the full-text is not changed in any way

The full-text must not be sold in any format or medium without the formal permission of the copyright holders.

Please consult the full DRO policy for further details.

Durham University Library, Stockton Road, Durham DH1 3LY, United Kingdom
Tel : +44 (0)191 334 3042 | Fax : +44 (0)191 334 2971
https://dro.dur.ac.uk

Available online at www.sciencedirect.com

ScienceDirect

journal homepage: www.elsevier.com/locate/he

Evaluation of performance characteristics of a novel hydrogen-fuelled free-piston engine generator

Ugochukwu Ngwaka [a], *Andrew Smallbone* [b,*], *Boru Jia* [c], *Christopher Lawrence* [b], *Ben Towell* [a], *Sumit Roy* [b], *Shivaprasad KV* [b], *Anthony Paul Roskilly* [b]

[a] *Sir Joseph Swan Centre for Energy Research, Newcastle University, Newcastle-upon-Tyne, NE1 7RU, UK*
[b] *Department of Engineering, Durham University, Durham, DH1 3LE, UK*
[c] *School of Mechanical Engineering, Beijing Institute of Technology, Beijing 100081, China*

HIGHLIGHTS

- Experimental results from hydrogen powered free piston engine generator.
- Comparison of results from two-stroke and four-stroke mode of operations.
- For similar operating conditions four-stroke performed better than two-stroke mode.
- Maximum power output was 650 W with negligible NOx emission.

GRAPHICAL ABSTRACT

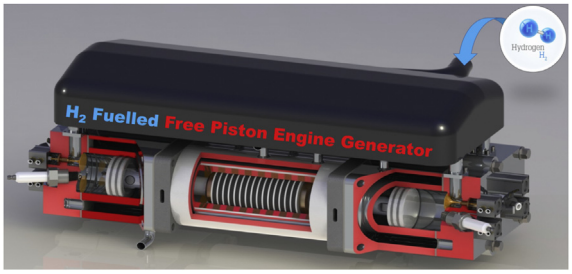

ARTICLE INFO

Article history:
Received 21 November 2019
Received in revised form
20 January 2020
Accepted 9 February 2020
Available online 12 March 2020

Keywords:
Free piston engine

ABSTRACT

In this work, we present the experimental results obtained from hydrogen fuelled spark-ignited dual piston free-piston engine generator (FPEG) prototype operated in two-stroke and four-stroke mode. The FPEG testing was successfully conducted at 3.7 compression ratio, engine speed between 5 Hz and 11 Hz and with different equivalence ratios. The FPEG technical details, experimental set-up and operational control are explained in detail. Performance indicators show that both equivalence ratio and engine speed affect the engine operation characteristics. For every set of specified FPEG parameters, appropriate range of equivalence ratio is recommended to prevent unwanted disturbance to electric generator operation. Both two-stroke and four-stroke cycle mode were tested, and the

Abbreviations: Bottom Dead Centre, BDC; Carbon Monoxide, CO; Exhaust Valve Closing, EVC; Exhaust Valve Opening, EVO; Free Piston Engine, FPE; Free Piston Engine Generator, FPEG; Free Piston Linear Generator, FPLG; Homogeneous Charge Compression Ignition, HCCI; Hybrid Electric Vehicle, HEV; Internal Combustion Engine, ICE; Indicated Mean Effective Pressure, iMEP; Intake Valve Closing, IVC; Intake Valve Opening, IVO; Mean Effective Pressure, MEP; Oxides of Nitrogen, NOx; Parts Per Million, ppm; Top Dead Centre, TDC; Standard Litre per minute, STL/min.

* *Corresponding author.*
E-mail address: andrew.smallbone@durham.ac.uk (A. Smallbone).

https://doi.org/10.1016/j.ijhydene.2020.02.072

0360-3199/© 2020 The Authors. Published by Elsevier Ltd on behalf of Hydrogen Energy Publications LLC. This is an open access article under the CC BY license (http://creativecommons.org/licenses/by/4.0/).

Electric vehicle range-extender
Hydrogen
Hydrogen combustion
Thermodynamic description
NOx emissions

results showed different combustion characteristics with the two thermodynamic cycles. Four-stroke cycle mode could operate with indicated thermal efficiency gain up to 13.2% compared with the two-stroke cycle.

© 2020 The Authors. Published by Elsevier Ltd on behalf of Hydrogen Energy Publications LLC. This is an open access article under the CC BY license (http://creativecommons.org/licenses/by/4.0/).

Introduction

In 2016, energy consumed by the transportation sector accounted for 19.5% of total world energy consumption [1] with crude oil-based fuels accounting for 94% [1,2]. World crude oil reserves are not infinite and the associated environmental impact of continuous use of crude oil-based fuels for transportation at the current rate is an international concern. Studies carried out by EXXONMOBIL [1] and BP [2] indicated that there will be a continuous growth in energy demands for transportation sector in the near future. At the current rate of consumption of crude oil-based fuels, the world crude oil reserves can only last for 50 years [3].

Consequently, some alternative automotive technologies have been proposed to tackle the environmental impact of emissions from crude oil-based fuels, and adopting alternative fuels is one of them [4]. Hydrogen is an alternative transportation fuel, it is the most abundant element on earth, and can therefore be considered as a potential "endless" energy source [5]. Hydrogen has the advantages of high efficiency and ultra-low emissions for internal combustion engine applications [6]. As a result of advantages offered by hydrogen fuel, it is considered by some as an ideal fuel to power arising technologies like the free-piston engine generator.

The free-piston engine generator (FPEG) is a linear internal combustion engine coupled with a linear electric generator. The FPEG considered in the present work is *dual piston* type. The piston assembly has a free linear motion between top dead centre (TDC) and bottom dead centre (BDC) and the piston assembly motion is controlled by gas and load forces acting upon it, therefore the requirement for a crankshaft mechanism is eliminated [7]. The FPEG has some advantages over traditional internal combustion engine (ICE). It has a simple mechanical structure with very few moving parts; this makes it compact with a high power-density [8]. A FPEG operates with a variable compression ratio; this makes the use of conventional gasoline fuel or alternative fuels such as hydrogen possible, and therefore can support emissions reduction without major hardware modifications [9].

Due to the elimination of crankshaft mechanism; there are no side forces between the piston and cylinder liner, and because fewer moving parts exist in FPEG, frictional losses are lower [10]. In free-piston engines, the piston can spend less time at TDC relative to the crank-shaft-driven piston, this shorter residence time at TDC could be attractive in terms of mitigating against heat transfer losses and NO*x* formation, because shorter time at higher temperature is desirable for lower heat transfer loss and less NO*x* formation [11,12].

Many engine researchers and developers are interested in using FPEG as an advanced power sources, which could offer increased performance and reduced emissions over conventional ICEs [13,14]. It is expected that the FPEG will suffer less thermal and machine losses compared with the current hybrid electric vehicle systems (HEVs) [15], and the prospects of high efficiency of a linear generator combined with the simple structures of a free-piston engine are prompting more interest in researchers towards FPEG development, especially for HEVs [13]. Configurations of FPEG can be categorised into four different types: single-piston engine configuration, dual-piston engine configuration, opposed-piston engine configuration and four-cylinder complex configuration [16]. In this research, a *first-of-its-kind* hydrogen-fuelled dual-piston FPEG is experimentally investigated in both two-stroke and four-stroke thermodynamic cycle.

The state-of-the-art

The concept of a modern free-piston engine was first proposed by Pescara [17] for air compression applications and a patent for spark ignition and compression ignition types were registered in 1925 and 1928 respectively. Recently there have been a renewed interest by researchers in development of FPEG and different research groups have reported on different prototypes model and experimental results.

Toyota Central Research and Development Labs Inc. reported stable operation of single-cylinder spark ignition FPEG prototype. This FPEG comprises a two-stroke combustion chamber at one end, a gas spring chamber at the opposite end and a linear generator configured in-between the combustion and gas spring chambers. In the course of the experiment, several abnormal combustion events were observed but the operation was reported to be continuously robust [18].

Researchers at West Virginia University presented the design and operation of a spark ignited dual-cylinder dual-piston FPEG prototype. The prototype was reported to have achieved 316 W power output at frequency of 23.1 Hz and 50 mm maximum stroke [19]. Nevertheless, researchers from Beijing Institute of Technology and Shanghai Jiao Tong University China developed a compression ignition dual-cylinder dual-piston FPEG prototype and a successful combustion was reported [20].

A Sandia National Laboratory research team [21] developed a single-cylinder opposed-piston FPEG prototype to investigate its potential use for HEVs. The opposed-piston FPEG prototype consisted of a centrally located combustion chamber, the linear generators were configured at each ends of the combustion chamber and two bounce chambers positioned at each ends of the generators. The prototype is driven from a

central combustion chamber, the bounce chamber served as energy storage to provide compression work for the next cycle. The prototype employed compression ignition combustion and hydrogen used as main fuel constituent. A successful low equivalence ratio (0.04–0.25) hydrogen homogenous charged compression ignition (HCCI) combustion was reported. However, hydrogen/air mixtures were ignited with compression ratios ranging from 20:1 up to 70:1. Indicated thermal efficiencies between 50% and 55% were reported. Due to some reported difficulties in controlling some engine parameters, the prototype operation proved insufficiently robust. Similarly, a two-stroke dual-cylinder dual-piston FPEG prototype was experimentally investigated on performance of hydrogen in HCCI mode [22]. It was reported that at compression ratio between 17 and 50, equivalence ratio of 0.319 and initial charge temperature of 22 °C, the engine achieves a cycle thermal efficiency of 55%. The exhaust analysis indicated NO_x emission less than 500 ppm and CO less than 40 ppm. The major cause of this high thermal efficiency is nearly constant volume combustion at high compression ratio [22].

Woo and Lee at Korea Institute of Energy Research developed and investigated the performance characteristics of a hydrogen fuelled two-stroke spark-ignited FPEG, the prototype is of dual-cylinder dual-piston configuration. The researchers adopted the so-called reverse uniflow scavenging and the prototype was successfully operated at 25 Hz. It was suggested that to have a reliable and stable operations in FPEG, a viable control system is needed to address the uncertainty of piston motion. The reported results show that optimum power is achieved when fuel is supplied before the exhaust port opens and then the intake valve opens at BDC. The engine achieved power output above 13 MPa of IMEP [23].

Numerical model researches of hydrogen fuelled FPEG, exploring different combustion methods have been also presented. A research team at Chongqing Jiao Tong University, numerically investigated the performance of a spark-ignited hydrogen fuelled FPEG [24] and hydrogen fuelled FPEG with pilot-ignition technology [25]. The simulation results indicated that hydrogen fuelled free-piston engine moves with higher velocity and acceleration around the TDC, operates with higher peak combustion pressure and has a longer combustion duration compared to a corresponding conventional hydrogen engine. However, the simulation results show that in a spark-ignited FPEG, hydrogen combustion rate is slower and exhibits shorter ignition delay compared with pilot-ignited FPEG. The researchers posited that rapid hydrogen combustion in pilot ignited FPEG will enhance the level of constant volume heat release around the TDC, this results in more indicated work and higher indicated thermal efficiency. The pilot-ignited FPEG favours higher system frequency, higher compression ratio, more power generation, as well as more NO_x emission compared with the spark-ignited system [25].

Zhang and Sun [5] numerically studied trajectory-based combustion control for hydrogen fuelled FPEG. The researchers adopted HCCI combustion and established that the minimal engine compression ratio to ignite hydrogen fuel in a trajectory based HCCI combustion is 22:1. Though, at optimised piston motion trajectories; based on higher work output and reduced emissions simultaneously as target, the results achieved engine thermal efficiency of 55.7% and NO_x emission less than 57 ppm.

In this work, we present the experimental set-up and first results obtained from a spark-ignited dual-piston FPEG operating with hydrogen fuelling in both two-stroke and four-stroke mode. It demonstrates the potential of operating with hydrogen fuel and the advantages and disadvantages of different thermodynamic gas-exchange cycles in FPEG. The performance, combustion and emissions characteristics were evaluated experimentally.

Experimental work

Instrumentation

Fig. 1 shows a schematic configuration of FPEG prototype and Fig. 2 is photograph of the actual prototype developed at Newcastle University. The main components are the internal combustion chambers and linear electric generator. The prototype is comprised of two internal combustion cylinders located at opposite ends, each with its corresponding combustion chamber. Each of the combustion chambers have independently controlled gas inlet and exhaust valves (labelled - 5 & 6), spark electrode (labelled - 1) and piston (labelled - 2). The linear electric machine (labelled - 8) which can be either operated as a motor or a generator is located between the two cylinders. The two pistons are rigidly connected using the piston-mover assembly (labelled - 7), the piston-mover assembly and is the only significant moving part of the system. Port fuel induction system (labelled - 9) was used to supply hydrogen fuel into the engine cylinder. During starting process, the linear electric machine runs as a motor, oscillating the piston-mover assembly until the air-fuel mixture in the combustion chamber attains the required conditions for spark-ignition. The linear electric machine continues to run as a motor until stable operation is achieved. However, once the engine is operating at steady-state the "motor" mode will be switched to "generator" mode. Combustion occurs alternatively in the combustion chambers and oscillates the piston-mover assembly. The oscillatory motion of the piston-mover assembly is converted into electrical energy by the linear electric generator. The inlet and exhaust valves are controlled by a linear actuated valve control system.

Many of the reported FPEG prototypes operate on a conventional two-stroke thermodynamic cycle. In dual-piston two-stroke FPEG configuration, the power stroke takes place alternately in each cylinder, and it drives the compression stroke of the other cylinder. However, this prototype configuration can operate in either two-stroke or four-stroke cycle by simply adjusting its control parameters. By adjusting the intake/exhaust valve timing, the working mode of the linear electric generator and carrying out the intake and compression strokes separately from the expansion and exhaust strokes, the FPEG prototype used can operate on either a two or four-stroke cycle.

In two-stroke cycle operation, compression and power strokes occur alternately in each cylinder and the linear

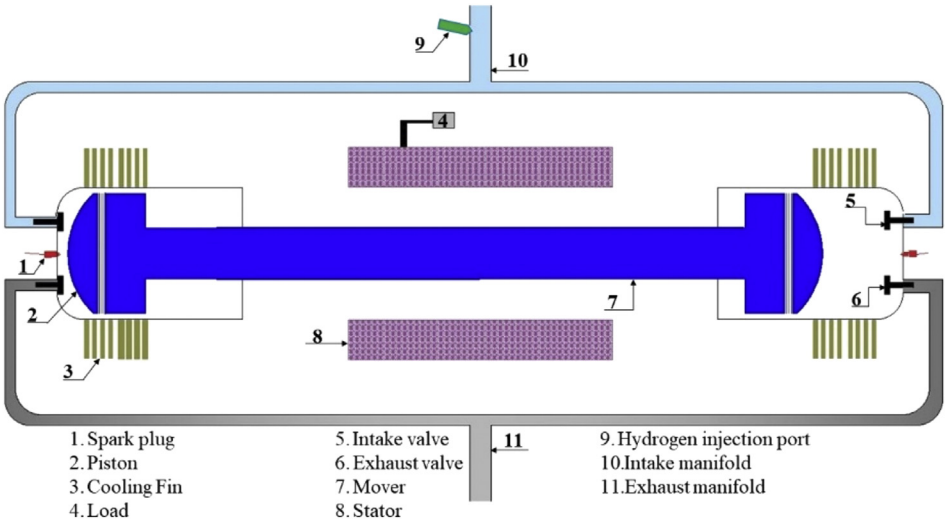

Fig. 1 – Prototype schematic configuration.

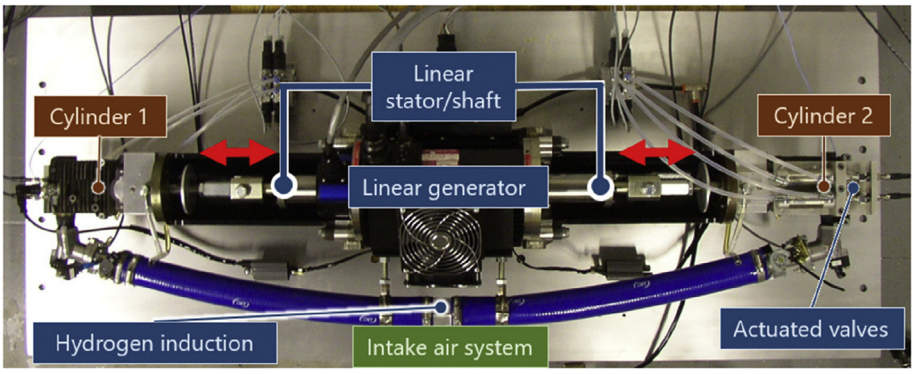

Fig. 2 – Actual FPEG prototype in Newcastle University.

electric generator is continuously operated as a generator all through the cycle.

1. Compression stroke: it is initiated when both intake and exhaust valves are closed, the air–fuel mixture in the cylinder is compressed until it attains the required compression ratio. The power stroke starts towards the end of compression stroke and the timing of combustion is initiated using a timed spark event, the spark ignites the air–fuel mixture and expansion follows.
2. Expansion stroke: the piston-mover assembly is forced to move backwards by the high-pressure expanding gas; this backward movement of the piston-mover assembly leads to compression in the opposite cylinder. The exhaust valves are opened towards the end of power stroke and the burnt gas exits the cylinder. The intake valves are opened at BDC and fresh charge is drawn into the cylinder.

The four-stroke thermodynamic cycle of FPEG is similar in principle with a traditional four-stroke engine, where each cylinder requires a total of four strokes to complete a single power stroke. Four-stroke operation in a FPEG comprises four different processes in the following sequence:

1. Intake stroke: it commences when the piston approaches TDC and the intake valves are opened, the stroke is completed by closing the intake valves when the piston is at BDC.
2. Compression stroke: compression stroke is initiated at BDC when both the intake and exhaust valves are closed. The air–fuel mixture in the cylinder is compressed until it attains the required conditions for ignition or required engine compression ratio at TDC with initiation of spark and flame propagation.
3. Power stroke: the high pressure burnt gases drives the piston-mover assembly from TDC towards BDC, and the linear electric generator converts part of the kinetic energy of the piston-mover assembly to electricity.
4. Exhaust stroke: this stroke is initiated by opening exhaust valves at BDC and is terminated when the exhaust valve is closed at TDC.

In a dual-cylinder FPEG operating in two-stroke mode, there are two power strokes in every oscillating cycle, therefore the electric machine generally works as a generator. However, in the same configuration in four-stroke mode, there is only one single power stroke in every oscillating cycle.

Consequently, electricity is produced only during the power stroke and the linear electric machine works as a motor to drive the non-power strokes. The comparison of two-stroke and four-stroke cycles sequence of steps for each cylinder and the corresponding mode of operation of the linear electric generator are summarised in Table 1.

Experimental procedure

The specifications of the FPEG are given in Table 2.

The experimental methodology can be summarised as follows:

1. Valve timing: The intake and exhaust valves are of poppet valve type with adjustable lift, an electro-pneumatic system based on a Festo actuator is employed to control the opening and closing timing of the intake and exhaust valves. This valve actuation system has been tested successfully, with a less than 8 ms opening latency (signal to being fully open) and a 20 ms closing latency. This means that the FPEG system can operate with valves with operational speeds in excess of 10–15 Hz.
2. Gas flowrate were controlled using thermal mass flow meters fed by the laboratory compressed airline (6 bar) and a 200-L hydrogen tank. The flowmeters were supplied by Aalborg at 50 l/min (GFC37) for hydrogen and 500 l/min (GFC67) for air. Well upstream of the intake ducts, the hydrogen and air were mixed to the desired air/fuel composition.
3. Piston position and electric machine control: The piston positions were measured using a variable inductor displacement sensors and encoder attached to the mover magnet inside the linear generator. A Moog linear motor (Model 50204D) was used for an electrical machine, this selection was mainly based on its capability to provide sufficient force during the starting process. A Parker model Compax3H was used as the motor drive, this system needed to be configured using C3 Manager Software via RS232 connection via a master computer. The motor was driven via a sinusoidal electrical commutation of three-phase coils. The mover's position, velocity, and acceleration information are provided by the linear encoder, and these were used as feedback to the mover's master control system.
4. In-cylinder pressure: The dynamic in-cylinder combustion chamber pressures were measured by AVL (Model ZI21) piezoelectric transducers sensors mounted in Bosch-supplied spark plugs.
5. The ignition system used in this prototype is a capacitor discharge ignition system, which consists of a 12 V battery, oscillator-transformer-rectifier circuit, capacitor, coil, and spark plug. The 12 V battery is stepped to high voltage (20 kV) by the ignition system.
6. Temperatures: Combustion chamber intake and exhaust temperatures were measured with type K thermocouples.
7. Emissions: Emissions were measured using a Testo 350-XL exhaust gas analyser and mainly focused on the quantification of nitrous oxides.
8. Data acquisition and control: These were implemented using the National Instrument CompactRIO system, the program for monitoring, control and display of the real-time signals is developed in LabVIEW. All actuators and sensors are connected to I/O modules on the CompactRIO system for data collection. The collected data is temporarily stored in the CompactRIO memory and then streamed to the host PC. The measured piston displacement and combustion chamber pressure were used as feedback signals to control the intake and exhaust valve timings. Data analysis were performed using a MATLAB script written to read measurements and scale the measured quantity to basic engineering units.
9. Performance calculations: the indicated work is computed as the integral of measured in-cylinder pressure and volume in both cylinders per cycle. The indicated efficiency is calculated as indicated work per cycle divided by the fuel energy delivered per cycle while the indicated power is calculated as the rate of work done per cycle.

Table 2 – FPEG prototype specifications.

Parameters [Unit]	Value
Moving mass [kg]	7.0
Maximum stroke [mm]	40.0
Actual stroke [mm]	34.0
Effective bore [mm]	50.0
Intake valve diameter [mm]	20.0
Exhaust valve diameter [mm]	18.0
Valve lift [mm]	4.0
Number of cylinders [–]	2
Nominal target compression ratio	3.7

Results and discussion

A conservative approach was adopted in the selection of the prototype piston stroke and engine speed, this was done to minimise the risk of impact between valves, the piston head and the cylinder end and to support the improved control strategy adopted. The linear electric machine was used as an active controller to control the piston movement according to

Table 1 – Comparison of two-stroke and four-stroke engine cycles.

	Two-stroke			Four-stroke		
	Right cylinder	Left cylinder	Linear machine	Right cylinder	Left cylinder	Linear machine
Stroke →	gas exchange + compression	power + gas exchange	generator	air intake	air exhaust	motor
Stroke ←	power + gas exchange	gas exchange + compression	generator	compression	air intake	motor
Stroke →	gas exchange + compression	power + gas exchange	generator	power	compression	generator
Stroke ←	power + gas exchange	gas exchange + compression	generator	air exhaust	power	generator

a pre-set sinusoidal displacement profile. The target piston displacement profile is a sinusoidal wave function with amplitudes of 17.0 mm and −17.0 mm. The pre-set piston stroke is 34.0 mm, the clearance from the cylinder head yielded a corresponding compression ratio of 3.7. An operating speed of 5 Hz was selected for the testing, which corresponds to 300 cycles per minute. The FPEG prototype was operated according to both two-stroke and four-stroke thermodynamic cycle; the valve timings and spark ignition initiation were controlled based on piston displacement and velocity feedback. During a series of engine tests, data were collected over 30–60 consecutive sequential combustion cycles and post-processed. The baseline operating parameters are set out in Table 3.

Two-stroke operation – influence of equivalence ratio

Combustion analysis

The in-cylinder pressure development, spark initiation event and valve timing events for a complete two-stroke cycle at engine operating frequency of 5 Hz, air supply at 120 STL/min and hydrogen supply at 22 STL/min are shown in Fig. 3a. While Fig. 3b shows the mean in-cylinder pressure, spark initiation event and valves operation with percentage of piston's total swept volume for a complete two-stroke cycle with the same operating parameters as Fig. 3a. The in-cylinder peak pressure position is the point of maximum conversion of fuel chemical energy to mechanical energy in FPEG, for optimal energy conversion and improved engine efficiency, the position of in-cylinder peak pressure to the piston TDC is important. It is desirable for the peak pressure position to be very close to the TDC during power stroke. The mean in-cylinder pressure for a complete two-stroke cycle at different equivalence ratios are shown in Fig. 3c. It is evident from Fig. 3c that the higher the equivalence ratio, the closer is the in-cylinder peak pressure position to the TDC in power stroke. Lower equivalence ratio results in a lower in-cylinder pressure values, whereas their pressure peaks are attained further away from TDC in power stroke when compared with higher equivalence ratio. A slight difference on the duration of combustion and ignition delay were found at different equivalent ratio, it can be observed in Fig. 3c, that combustion is more rapid at higher equivalence ratio when compared to lower equivalence ratio scenario. The ignition delay is shorter in higher equivalence ratio combustion and longer in lower equivalence ratio combustion (Fig. 3c). For complete fuel combustion and optimal energy conversion, it is desirable for the combustion to start very close to the piston TDC in the power stroke. It can be seen in cases of higher equivalence ratio that combustion occurs closer to the piston TDC and further away from the TDC at lower equivalence ratio.

The piston velocity and displacement profiles are shown in Fig. 3d for different equivalence ratios. As noted in Fig. 3c, the magnitude of peak in-cylinder pressure is proportional to the equivalence ratio. The in-cylinder gas pressure forces exerted on the piston is proportional to the equivalence ratio, this can be observed in piston position profile deviation from a pre-set position profile immediately after TDC in Fig. 3d and this deviation from a pre-set position profile leads to a surge in piston velocity after the TDC. This sharp increase in piston velocity is proportional to the equivalence ratio. It implies that the linear generator will extract more power to counter the surge in piston velocity and to maintain the pre-set displacement profile. The response of the linear generator due to velocity surge is observed by the sudden drop in piston velocity just after the surge (Fig. 3d). The surge in piston velocity is a disturbance to the electric generator operation; therefore, an optimised equivalence ratio for a set of engine parameters is required for a smooth operation of the engine.

Performance analysis

The influence of equivalence ratio (hydrogen fuel loading) on the performance of FPEG prototype operated in two-stroke mode at frequency of 5 Hz are evaluated and presented in this section. The in-cylinder peak pressure at different hydrogen flow rates (fuel-air equivalence ratios) for a two-stroke thermodynamic cycle is shown in Fig. 4a. The in-cylinder peak pressure value increases with increase in equivalence ratio. With higher equivalence ratio, the peak pressure in the combustion chamber is found to be higher and shows a linear relationship with the equivalence ratio. This is expected because the quantity of fuel supplied to the combustion chambers translates to energy available after combustion because of superior burning properties of hydrogen fuel. Fig. 4b shows the peak pressure timing at different equivalence ratios. It is important to note that the spark initiation event occurs at the same timing irrelevant of the equivalence ratio. The time it takes for the in-cylinder pressure to attain maximum pressure has a negative correlation to the equivalent ratio: with higher equivalence ratio, the combustion chamber peak pressure timing is found to be lower and shows a negative linear relationship with the equivalence ratio. It is evident from Figs. 3c and 4a that higher equivalence ratio results in higher in-cylinder peak pressure value. We found that the combustion become more stable from equivalence ratio of 0.4365 (22 STL/min hydrogen flowrate) and above as apparent from Fig. 4b; the level of fluctuations on the peak pressure timing at 0.4365 equivalence ratio and above start to decrease when compared to the earlier equivalence ratios. Less variations on peak pressure timing is an indication that shows that combustion is more stable.

Table 3 – Main operating parameters.

Parameters [Unit]	Value	
Operational speed [Hz]	5.0	
Reference Position (Ref) [mm]	15.0	
	Two-stroke	Four-stroke
Top Dead Centre (TDC) [s aRef]	0.059	0.064
Bottom Dead Centre (BDC) [s aRef]	0.160	0.163
Spark Timing [s aTDC]	−0.014	−0.021
Inlet Valve Open (IVO) [s aTDC]	−0.034	−0.017
Inlet Valve Close (IVC) [s aTDC]	0.006	0.114
Exhaust Valve Open (EVO) [s aBDC]	0.039	−0.009
Exhaust Valve Close (EVC) [s aBDC]	0.077	0.112

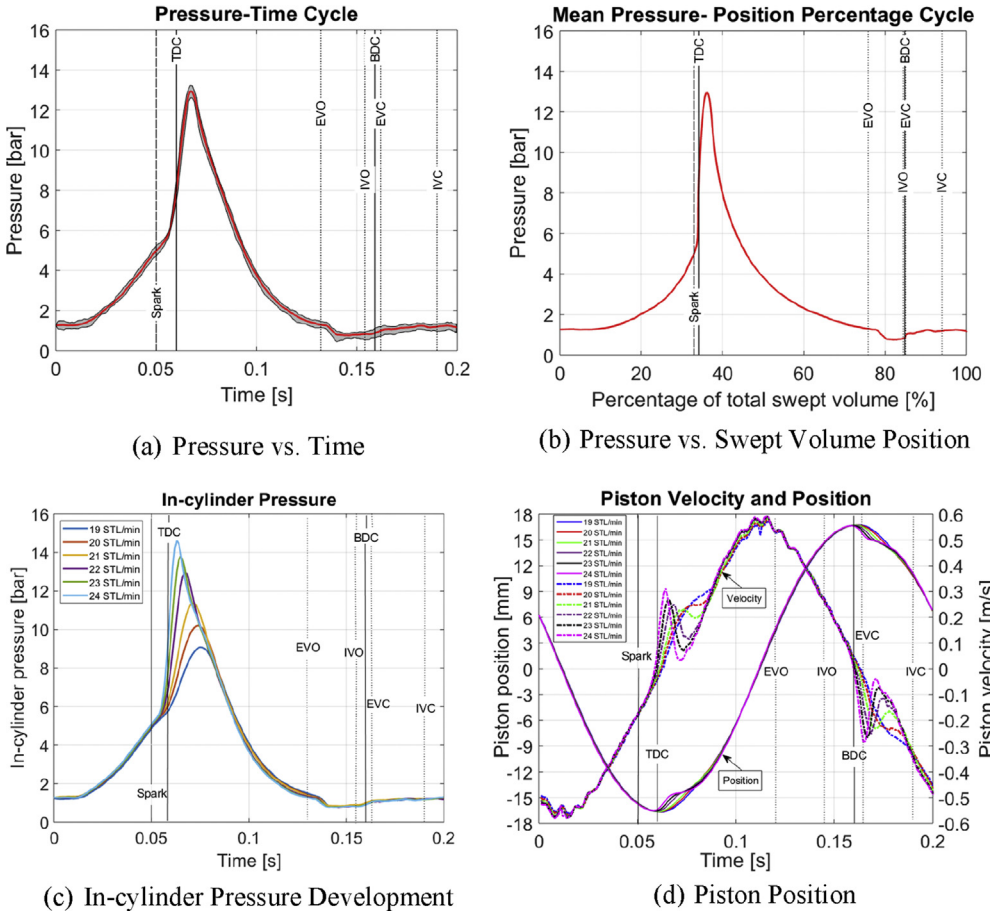

Fig. 3 – In-cylinder pressure development for two-stroke cycle mode.

The relationship between work done and indicated efficiency with varying equivalence ratio are shown in Fig. 4c and 4d respectively. It is expected that with higher equivalence ratio, the work done will be higher and that work done will exhibit a linear relationship with the equivalence ratio. Rather the work done was found to be nearly a constant irrespective of the equivalence ratio. The engine indicated efficiency drops gradually despite having a higher peak in-cylinder pressure at higher equivalent ratio. With higher equivalence ratio, the indicated efficiency is found to be lower, and shows a negative linear relationship with the equivalence ratio. Maximum indicated efficiency obtained for two-stroke cycle was 32.3% at 0.377 equivalence ratio, corresponding to 19 STL/min hydrogen flowrate. The results show that the equivalence ratio has a significant effect on the performance of FPEG.

Four-stroke operation– influence of increasing speed

Combustion analysis

The in-cylinder pressure development, spark initiation event and valve timing events for complete four-stroke cycle are shown in Fig. 5a. While Fig. 5b shows the mean in-cylinder pressure, spark initiation event and valves operation with percentage of piston's total swept volume for a complete four-stroke cycle mode of operation. In-cylinder pressure profile is among the important parameters in thermodynamic analysis of internal combustion engine, and it is a typical indicator of the combustion process, which can be used to evaluate the efficiency of chemical to mechanical energy conversion in the engine.

Performance analysis

The FPEG prototype is further investigated to understand the impact of varying frequency (speed) on system performance. The effects of operational frequency on peak pressure, peak pressure timing, indicated work, indicated power and indicated efficiency at equivalence ratio of 0.4365 (at 11 STL/min hydrogen flowrate and 60 STL/min air flowrate) are presented in Fig. 6. The operating frequency was varied from the operational base frequency of 5 Hz–11 Hz, while the other FPEG operational variables were kept the same. Increase in operating frequency lead to a decrease in magnitude of peak pressure as seen in Fig. 6a. This behaviour is expected because less quantity of fuel is available for combustion at every frequency increment when the fuel flowrate is constant. Fuel content in the combustion chamber is proportional to the energy content from combustion gases; which in this case, is indicated by the in-cylinder pressure. The

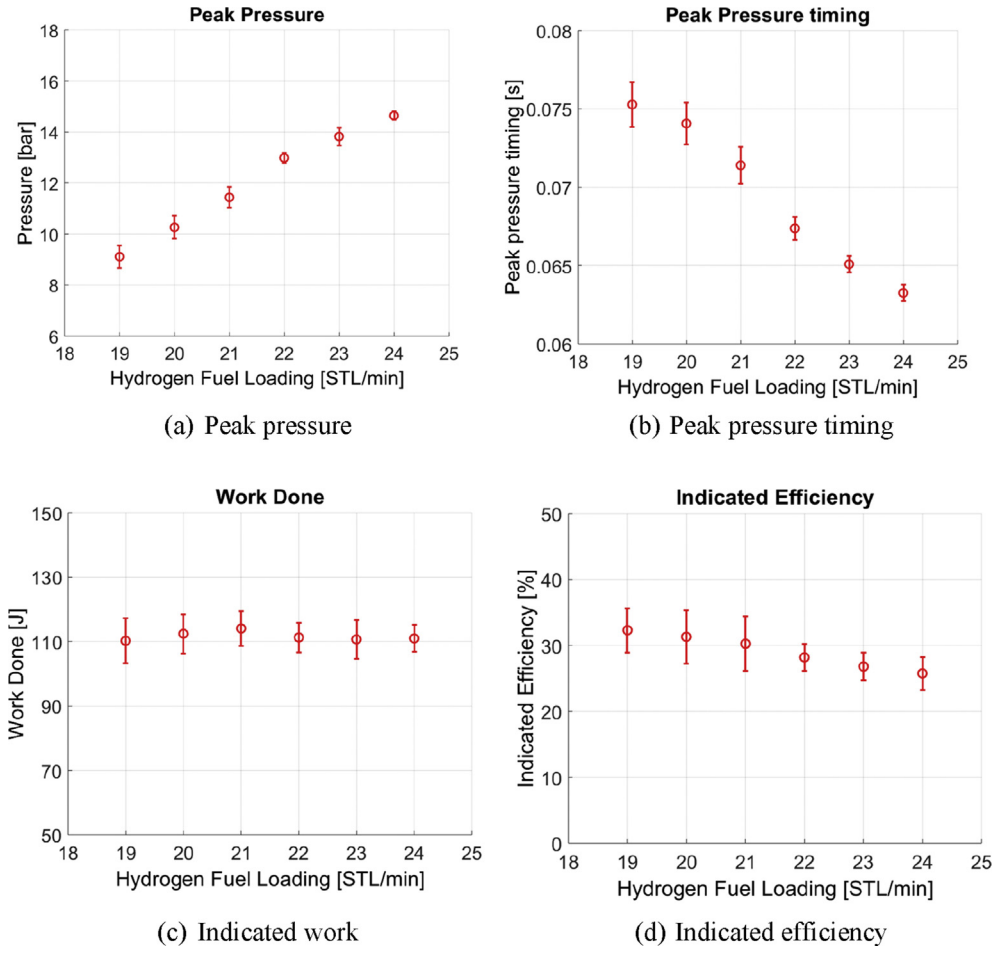

Fig. 4 – Impact of equivalence ratio on performance for two-stroke cycle mode.

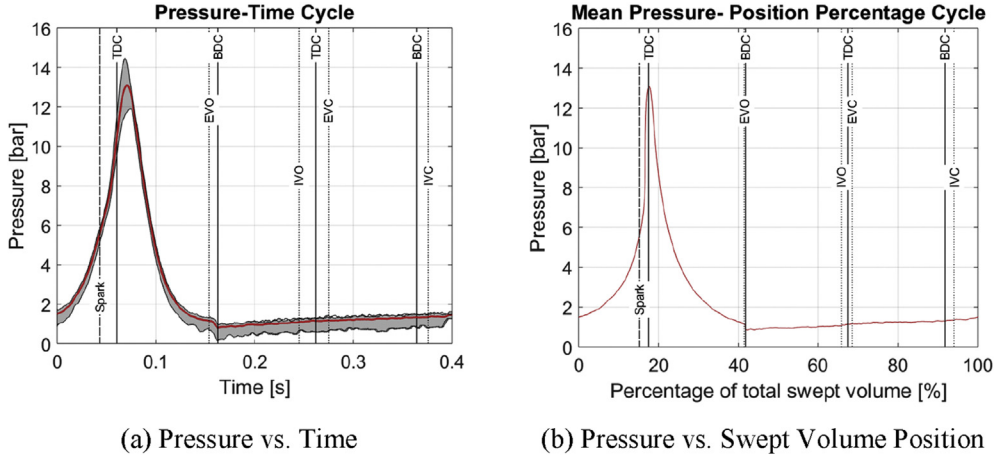

Fig. 5 – In-cylinder pressure development for four-stroke cycle mode.

peak pressure timing (Fig. 6b) decreases with increase in frequency, it is expected that the peak pressure timing will increase when the quantity of fuel available for combustion become lesser in cases of increased frequency but rather the opposite trend is observed, this is due to influence of increased engine speed on FPEG combustion. Indicated work and indicated efficiency decreased as the frequency increased as shown in Fig. 6c and 6e respectively, however the indicated power increased with increase in operational frequency (Fig. 6d). The highest indicated efficiency achieved for four-stroke cycle was 45.5% at 6 Hz, which was 13.2% greater than the indicated efficiency achieved for two-stroke

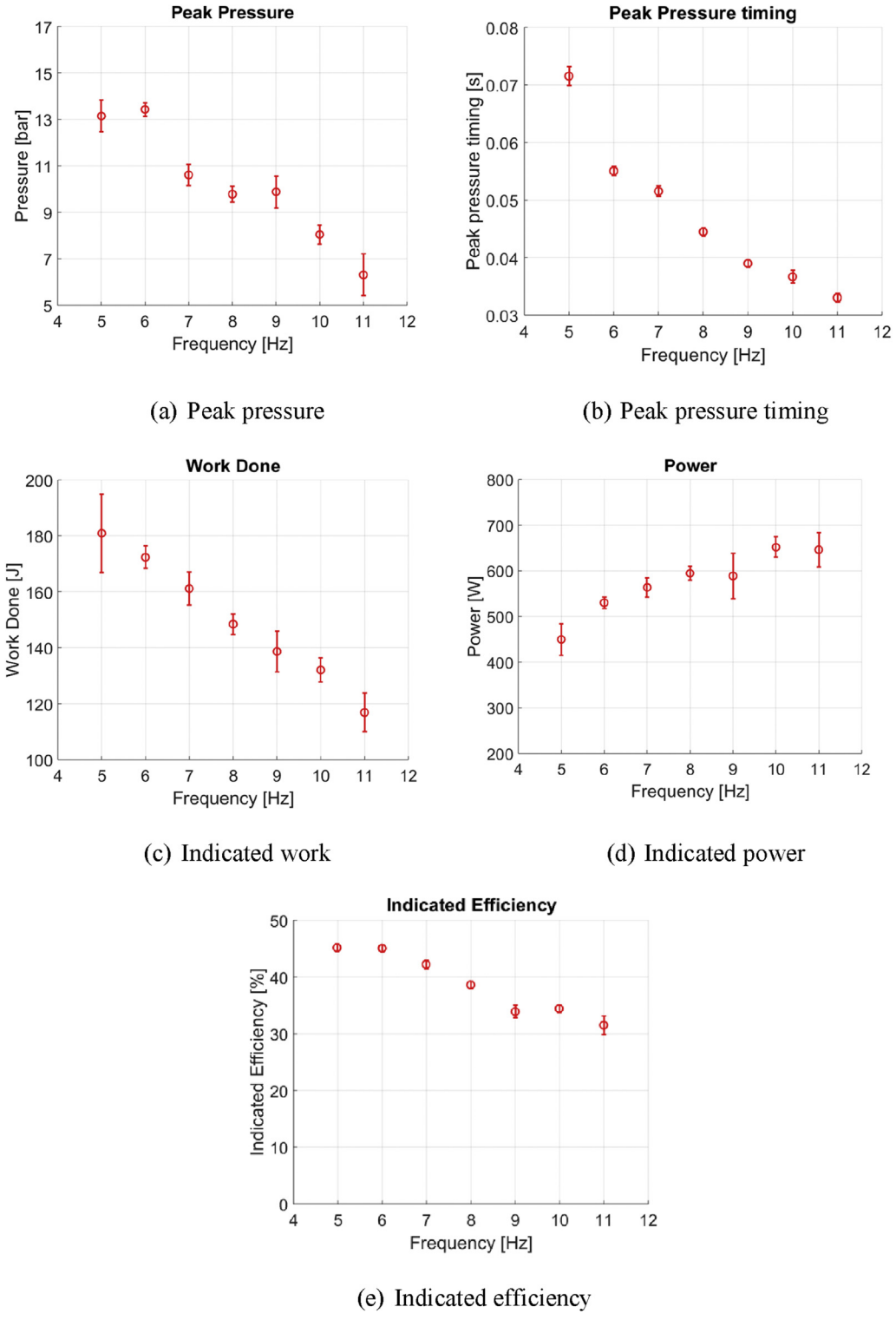

Fig. 6 – Influence of speed on performance for four-stroke cycle mode.

cycle mode. An increase in indicated power output and decrease in indicated efficiency was observed as a function of increasing frequency (operating speed) this is most likely associated with a reduction in the efficiency of the gas exchange process. This was because the control system fixed the valve timing signal time, however in practice there is a real-time delay in this actuation. Thus with increasing speed, the fixed valve timing needs there is scope for further optimisation. The FPEG achieved power output of 650 W at 11 Hz.

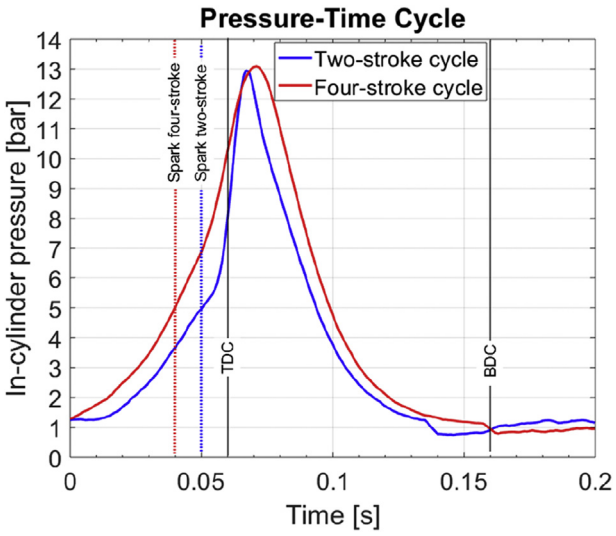

Fig. 7 – Pressure development in a mean two-stroke and four-stroke cycle.

Comparison of in-cylinder pressure development in two and four-stroke mode of operation

The in-cylinder pressure for a two-stroke thermodynamic cycle and in-cylinder pressure during compression stroke and power stroke for a four-stroke thermodynamic cycle are shown in Fig. 7. The both cycles (two thermodynamic cycles) were operated at the same equivalence ratio of 0.4365 and frequency of 5 Hz. Spark initiation event is programed to commence when the in-cylinder charge reaches a pre-set threshold of 5 bar, both in the two-stroke and the four-stroke thermodynamic cycle. The four-stroke cycle mode exhibits slightly higher peak in-cylinder pressure and higher overall in-cylinder pressure from the peak pressure position to the BDC when compared to the two-stroke cycle mode. It can be observed that combustion is longer in four-stroke cycle compared to the two-stroke cycle, and the reason for higher in-cylinder combustion pressure and longer combustion time observed in four-stroke cycle is because of superior charge mixture capability and higher scavenging efficiency inherit in four-stroke cycle process. In four-stroke mode, the FPEG produced 13% more indicated efficiency as compared to two-stroke mode of operation. The outcome of lower efficiency in two stroke than in four stroke mode also confirmed by the Woo and Lee in one of their FPEG research paper [23].

Emission from FPEG

This section describes the emission characteristic of FPEG in two-stroke and four-stroke mode of operation with the use of hydrogen fuel. The chemical reaction of hydrogen fuel and air leads to complete combustion with the release of heat along with water vapour and nitrogen oxides as a main pollutant. Engine out NOx emissions are plotted in Fig. 8. The nitrogen oxides emission analysis from the FPEG at operating frequency of 5 Hz and equivalence ratio of 0.4365 is shown in the figure. The two-stroke mode of FPEG produces NOx emission of 44 ppm, which is lesser than the four-stroke mode NOx emission of 84 ppm. This is mainly due to in-cylinder temperature, which is more in four-stroke cycle than two-stroke cycle. It further confirms that at equivalence ratio below 0.5; that is the NO_X emissions critical limit, NO_X emissions from hydrogen combustion in internal combustion engine is extremely low without implementing any after-treatment measures [26]. The low NO_X emission can be attributed to the relatively low engine compression ratio of 3.7, which gives rise to low temperature combustion. The similar trend of low NO_X emission in free-piston hydrogen engine generator has been reported by Yuan et al. [24].

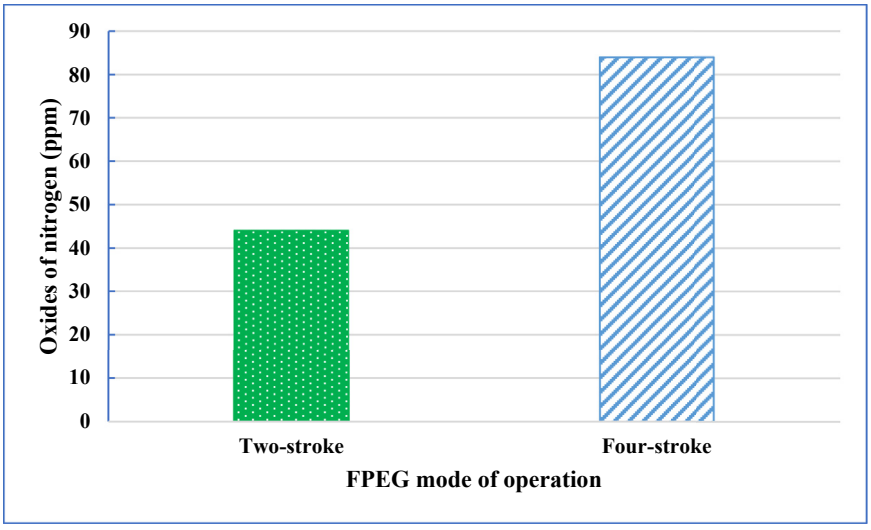

Fig. 8 – NOx emissions from FPEG.

Conclusions

In this paper, the experimental results obtained from hydrogen fuelled spark-ignited dual piston free-piston engine generator (FPEG) prototype operated in two-stroke and four-stroke mode are presented and analysed. It is found that:

- Performance indicators show that both equivalence ratio and engine speed affect the engine operation characteristics. The peak pressure value in the combustion chamber shows a positive linear relationship with the equivalence ratio, while the peak pressure timing shows a negative linear relationship with the equivalence ratio. Both the in-cylinder peak pressure and peak pressure timing shows a negative correlation with the engine speed.
- The results from both two-stroke and four-stroke cycle mode showed different combustion characteristics with the two thermodynamic cycles. Four-stroke cycle mode can operate with indicated thermal efficiency gain up to 13.2% compared with the two-stroke cycle.
- In every set of specified FPEG operation parameters, appropriate range of equivalence ratio is recommended to prevent unwanted disturbance to electric generator operation. The FPEG achieved maximum power output of 650 W at 11 Hz.
- The four-stroke mode of FPEG operation produces more NOx emissions compared to two-stroke mode of operation. The investigation also confirms that, the NOx emission is minimal at equivalence ratio less than 0.5.

Acknowledgement

This work was funded using the EPSRC (Engineering and Physical Sciences Research Council) (EP/R041970/1 and EP/S032134/1). Data supporting this publication are openly available under an Open Data Commons Open Database License at doi:10.15128/r144558d30v.

REFERENCES

[1] EXXONMOBIL. Outlook for energy: a view to 2040. 2018.
[2] BP. Energy outlook 2019. 2019.
[3] BP. BP statistical review of world energy 2018. 2018.
[4] Bae C, Kim J. Alternative fuels for internal combustion engines. Proc Combust Inst 2017;36:3389–413.
[5] Zhang C, Sun Z. Trajectory-based combustion control for renewable fuels in free piston engines. Appl Energy 2017;187:72–83.
[6] Karim GA. Hydrogen as a spark ignition engine fuel. Int J Hydrogen Energy 2003;28:569–77.
[7] Mikalsen R, Roskilly AP. The design and simulation of a two-stroke free-piston compression ignition engine for electrical power generation. Appl Therm Eng 2008;28:589–600.
[8] Wang Y, Chen L, Jia B, Roskilly AP. Experimental study of the operation characteristics of an air-driven free-piston linear expander. Appl Energy 2017;195:93–9.
[9] Mikalsen R, Roskilly AP. A review of free-piston engine history and applications. Appl Therm Eng 2007;27:2339–52.
[10] Ngwaka U, Jia B, Lawrence C, Wu D, Smallbone A, Roskilly AP. The characteristics of a Linear Joule Engine Generator operating on a dry friction principle. Appl Energy 2019;237:49–59.
[11] Goldsborough SS, Van Blarigan P. Optimizing the scavenging system for a two-stroke cycle, free piston engine for high efficiency and low emissions: a computational approach. SAE Trans 2003;112:1–20.
[12] Jia B, Wang Y, Smallbone A, Roskilly PA. Analysis of the scavenging process of a two-stroke free-piston engine based on the selection of scavenging ports or valves. Energies 2018;11.
[13] Hung NB, Lim O. A review of free-piston linear engines. Appl Energy 2016;178:78–97.
[14] Jia B, Smallbone A, Zuo Z, Feng H, Roskilly AP. Design and simulation of a two- or four-stroke free-piston engine generator for range extender applications. Energy Convers Manag 2016;111:289–98.
[15] Sato M, Nirei M, Yamanaka Y, Murata H, Bu Y, Mizuno T. Operation range of generation braking force to achieve high efficiency considering combustion in a free-piston engine linear generator system. IEEJ J Indust Applic 2018;7:343–50.
[16] Hung NB, Lim O, Iida N. The effects of key parameters on the transition from SI combustion to HCCI combustion in a two-stroke free piston linear engine. Appl Energy 2015;137:385–401.
[17] Pescara RP. Motor Compr Apparat 1928;1:657. 641. In: Office USP, editor. United States.
[18] Kosaka H, Akita T, Moriya K, Goto S, Hotta Y, Umeno T, et al. Development of free piston engine linear generator system part 1 - investigation of fundamental characteristics. SAE International; 2014.
[19] Subhash N. Two-stroke linear engine: Dissertation. West Virginia University; 1998.
[20] Yuan C, Feng H, He Y. An experimental research on the combustion and heat release characteristics of a free-piston diesel engine generator. Fuel 2017;188:390–400.
[21] Johnson TA, Leick MT, Moses RW. Experimental evaluation of the free piston engine-linear alternator (FPLA). Albuquerque, NM, USA: Sandia National Laboratories; 2015.
[22] Van Blarigan P, Paradiso N, Goldsborough S. Homogeneous charge compression ignition with a free piston: a new approach to ideal otto cycle performance. SAE International; 1998.
[23] Woo Y, Lee YJ. Free piston engine generator: technology review and an experimental evaluation with hydrogen fuel. Int J Automot Technol 2014;15:229–35.
[24] Yuan C, Xu J, He Y. Performance characteristics analysis of a hydrogen fueled free-piston engine generator. Int J Hydrogen Energy 2016;41:3259–71.
[25] Yuan C, Han C, Xu J. Numerical evaluation of pilot-ignition technology used for a hydrogen fuelled free piston engine generator. Int J Hydrogen Energy 2017;42:28599–611.
[26] Verhelst S, Wallner T, Sierens R. Hydrogen-Fueled internal combustion engines. Handbook of hydrogen energy. CRC Press; 2014. p. 840–921.